Top-quark FCNC productions at CERN LHC in topcolor-assisted technicolor model

Junjie Cao,[1,2] Guoli Liu,[3] Jin Min Yang,[4] and Huanjun Zhang[1,4]

[1]*Department of Physics, Henan Normal University, Xinxiang 453007, China*
[2]*Physics Department, Technion, 32000 Haifa, Israel*
[3]*Service de Physique Theorique CP225, Universite Libre de Bruxelles, 1050 Brussels, Belgium*
[4]*Institute of Theoretical Physics, Academia Sinica, Beijing 100080, China*

(Received 29 March 2007; published 12 July 2007)

We evaluate the top-quark FCNC productions induced by the topcolor-assisted technicolor (TC2) model at the LHC. These productions proceed, respectively, through the parton-level processes $gg \to t\bar{c}$, $cg \to t$, $cg \to tg$, $cg \to tZ$, and $cg \to t\gamma$. We show the dependence of the production rates on the relevant TC2 parameters and compare the results with the predictions in the minimal supersymmetric model. We find that for each channel the TC2 model allows for a much larger production rate than the supersymmetric model. All these rare productions in the TC2 model can be enhanced above the 3σ sensitivity of the LHC. Since in the minimal supersymmetric model only $cg \to t$ is slightly larger than the corresponding LHC sensitivity, the observation of these processes will favor the TC2 model over the supersymmetric model. In case of unobservation, the LHC can set meaningful constraints on the TC2 parameters.

DOI: 10.1103/PhysRevD.76.014004 PACS numbers: 14.65.Ha, 12.60.Fr, 12.60.Jv

I. INTRODUCTION

It is well known that flavor-changing neutral-current (FCNC) processes have been a crucial test for the standard model (SM) and a good probe for new physics beyond the SM. As the heaviest fermion in the SM, the top quark may play a special role in such FCNC phenomenology. In the SM the top-quark FCNC interactions are extremely suppressed [1] and impossible to be detected in current and foreseeable colliders. In contrast to the SM, the new physics models often predict much larger FCNC top-quark interactions [2]. Such large FCNC top-quark interactions are so far allowed by current experiments since the Tevatron collider only gave some rather loose bounds on the FCNC top-quark decays due to the small statistics [3]. The future colliders like the LHC will allow a precision test for the top-quark properties including the FCNC interactions [4].

Once the measurement of the FCNC top-quark processes is performed at the LHC, some new physics models can be immediately tested. For example, the FCNC top-quark decays and top-charm associated productions were found to be significantly enhanced in the minimal supersymmetric model [5,6] and technicolor models [7,8].

Although so far in the literature there are many papers devoted to the new physics contributions to the FCNC top-quark productions at the LHC, usually different processes are treated in different papers. Since these FCNC processes are correlated in a given new physics model, it is necessary to give a comprehensive study of all these processes in one paper. Recently, such an effort was given for the popular supersymmetric models [9]. In this work we perform a comprehensive analysis for the FCNC top-quark productions in the TC2 model. We will consider the production channels

$$gg \to t\bar{c}, \qquad cg \to t, \qquad cg \to tg, \qquad cg \to tZ, \qquad cg \to t\gamma. \tag{1}$$

Some of these processes have been studied in the literature: $gg \to t\bar{c}$ was studied in the second and third papers in [7], but only the s-channel contributions were considered; $cg \to tV$ (V is a vector boson) were studied in [10], but all box diagrams were ignored. The other process $cg \to t$ in the TC2 model has not been studied in the literature. In this work we consider all these productions and compare their rates. Also, we will compare the TC2 results with the predictions of supersymmetric models. Note that in our studies the parton-level processes will be used to label the corresponding hadronic productions and the charge-conjugate channel for each production is also included.

II. ABOUT TC2 MODEL

Before our calculations we recapitulate the basics of the TC2 model. As is well known, the fancy idea of technicolor tries to provide an elegant dynamical mechanism for electroweak symmetry breaking, but it encounters great difficulty when trying to generate fermion masses, especially the heavy top-quark mass. The TC2 model [11] combines technicolor interaction with top-color interaction, with the former being responsible for electroweak symmetry breaking and the latter for generating large top-quark mass. This model so far survives current experimental constraints and remains one of the candidates of new physics.

The TC2 model predicts a number of pseudo-Goldstone bosons like the top pions (π_t^0 and $\pi_t^{\pm}$) at the weak scale [11]. The top-quark interactions are altered with respect to the SM predictions since it is treated differently from other fermions in the TC2 model. For example, the TC2 model predicts some anomalous couplings for the top quark, such

as the tree-level FCNC coupling $t\bar{c}\pi_t^0$ and the charged-current $t\bar{b}\pi_t^-$ coupling given by

$$\begin{aligned}&\frac{(1-\epsilon)m_t}{\sqrt{2}F_t}\frac{\sqrt{v^2-F_t^2}}{v}(iK_{UL}^{tt}K_{UR}^{tt}\bar{t}_L t_R\pi_t^0\\&+\sqrt{2}K_{UR}^{tt}K_{DL}^{bb}\bar{t}_R b_L\pi_t^- + iK_{UL}^{tt}K_{UR}^{tc}\bar{t}_L c_R\pi_t^0\\&+\sqrt{2}K_{UR}^{tc}K_{DL}^{bb}\bar{c}_R b_L\pi_t^- + K_{UL}^{tt}K_{UR}^{tt}\bar{t}_L t_R h_t^0\\&+K_{UL}^{tt}K_{UR}^{tc}\bar{t}_L c_R h_t^0+\text{H.c.}),\end{aligned}\tag{2}$$

where the factor $\sqrt{v^2-F_t^2}/v$ ($v\simeq 174$ GeV) reflects the effect of the mixing between the top pions and the would-be Goldstone bosons [12]. K_{UL}, K_{DL}, and K_{UR} are the rotation matrices that transform, respectively, the weak eigenstates of left-handed up-type, down-type, and right-handed up-type quarks to their mass eigenstates. The TC2 model also predicts a CP-even scalar called top Higgs (h_t^0), whose couplings to top quark are similar to the neutral top pion [13].

One generic feature of top-condensation models such as the TC2 model is that the up-type quark mass matrix M_U exhibits an approximate triangular texture [14]. This character makes it possible to construct a realistic pattern of K_{UL} and K_{DL} such that (i) the Cabibbo-Kobayashi-Maskawa (CKM) matrix is reproduced, (ii) the Cabibbio mixing is mainly generated from K_{DL} while the mixing between the 3rd and 2nd families is mainly from K_{UL}, and (iii) all dangerous contributions to low energy observables such as $D^0-\bar{D}^0$ and $B^0-\bar{B}^0$ mixings as well as $b\to s\gamma$ can be evaded [13]. Numerically the quark flavor mixings are given as [13]

$$\begin{aligned}K_{UL}&\sim\begin{pmatrix}1 & 0 & 0\\ 0 & 1 & -0.033-0.014i\\ 0 & 0.033-0.014i & 1\end{pmatrix},\\ K_{DL}&\sim\begin{pmatrix}0.974 & 0.227 & 0.002-0.003i\\ -0.227 & 0.974 & 0.009-0.014i\\ 0 & -0.009-0.014i & 1\end{pmatrix}.\end{aligned}\tag{3}$$

Furthermore, a detailed analysis of K_{UR} indicates that the t_R-c_R mixing, K_{UR}^{tc}, can be naturally large, around $0.2\sim 0.3$. This is what we are interested in this paper. In our following analyses, we follow [13] to parametrize K_{UR}^{tt} as

$$K_{UR}^{tt}\simeq\frac{m_t'}{m_t}=1-\epsilon,\tag{4}$$

with m_t' denoting the top-color contribution to the top-quark mass, and by neglecting the mixing between right-handed up quark and right-handed top quark, we relate K_{UR}^{tc} with K_{UR}^{tt} by

$$K_{UR}^{tc}=\sqrt{1-(K_{UR}^{tt})^2}=\sqrt{2\epsilon-\epsilon^2}.\tag{5}$$

The parameters involved in our calculations are: the masses of the top pions and top Higgs, the parameter K_{UR}^{tc}, and the top-pion decay constant F_t. In our study we take $m_t=170.9$ GeV [15] and $F_t=50$ GeV. Since the mass splitting between neutral and charged top pion is very small, we assume $m_\pi^0=m_\pi^\pm$. The top pions mass is model dependent and is usually of a few hundred GeV [11]. About the top-Higgs mass, Ref. [7] gave a lower bound of about $2m_t$, but it is an approximate analysis and the mass below $t\bar{t}$ threshold is also possible [16]. In our analysis we assume

$$m_{\pi_t^0}=m_{\pi_t^\pm}=m_{h_t^0}\equiv M_{TC}.\tag{6}$$

Now we briefly review the low energy constraints on the TC2 model. (i) $D^0-\bar{D}^0$ mixing: In the TC2 model, the leading contribution comes from the exchange of a neutral top pion or top Higgs at tree level. This contribution is proportional to $(K_{UL}^{tu*}K_{UR}^{tc})^2$ and thus highly suppressed by very small K_{UL}^{tu} in Eq. (3). So $D^0-\bar{D}^0$ mixing can hardly set effective constraints on the TC2 model. In fact, as analyzed in [14], even in the naive $\sqrt{CKM}$-ansatz of the quark flavor mixing where $K_{UL}^{tu*}K_{UR}^{tc}\sim 10^{-4}$, a top-pion mass of $m_{\pi^0}=200$ GeV only contributes to $D^0-\bar{D}^0$ mass splitting by about 2×10^{-14} GeV, a factor of 2 below the current experimental limit of 4×10^{-14} GeV [17] (the SM prediction is smaller than 10^{-15} GeV). (ii) $B^0-\bar{B}^0$ mixing: Although at loop level the charged top pions can contribute to the mixings (such contributions are suppressed by loop factors and also by the small couplings of $\bar{c}d\pi^-$, $\bar{c}s\pi^-$, $\bar{t}d\pi^-$, and $\bar{t}s\pi^-$), the dominant effects are from the tree-level exchange of a bottom pion or bottom Higgs. Current experimental measurements of Δm_{B_d} and Δm_{B_s} imply [14]:

$$\begin{aligned}\frac{|K_{DL}^{bd}K_{DR}^{bd}|}{m_{H_b}^2}&<10^{-12}\ \text{GeV}^{-2},\\ \frac{|K_{DL}^{bs}K_{DR}^{bs}|}{m_{H_b}^2}&<10^{-10}\ \text{GeV}^{-2}.\end{aligned}\tag{7}$$

Thus, if $m_{H_b}^2$ is of the order of 1 TeV, then (7) imposes a stringent constraint on $K_{DL}^{bd}K_{DR}^{bd}$ and $K_{DL}^{bs}K_{DR}^{bs}$. However, considering the small values of K_{DL}^{bd} and K_{DL}^{bs} in Eq. (3), one sees that the triangular texture of the up quark mass matrix provides a nature alleviation for the constraints on K_{DR}^{bd} and K_{DR}^{bs}. (iii) $b\to s\gamma$: The TC2 contribution to this process mainly comes from the loops mediated by a charged top pion or a charged bottom pion. As shown in Figs. 2 and 3 in [14], these two kinds of contributions tend to cancel each other, and by setting the proper values of m_{H_b} and a small K_{DR}^{bs}, a top pion with a mass around the top-quark mass can still satisfy the experimental data. (iv) $b\to sl^+l^-$: As studied in [14], the TC2 model can greatly enhance the branching ratio for $b\to s\tau^+\tau^-$ via the tree-level exchange of Z' gauge boson, but for $b\to se^+e^-$ and $b\to s\mu^+\mu^-$ such a Z' contribution is much suppressed. So the current measurements of $b\to se^+e^-$ and $b\to s\mu^+\mu^-$ cannot set essential constraints on the TC2

theory [18]. (v) Constraints from R_b: In the TC2 model the dominant corrections to R_b come from the extended technicolor (ETC) gauge boson contribution as well as the charged top-pion contribution. If the ETC sector is the multiscale technioncolor (the so-called Model-II in the second reference of [19]), then for the typical parameters in the ETC sector, the charged top pion should be several hundred GeV [19]. For $\epsilon \sim 0.08$, which approximately corresponds to the case in our analyses, the top-pion mass should be larger than 250 GeV [19].

III. CALCULATIONS

For the parton-level processes in Eq. (1) we only plot the Feynman diagrams in Figs. 1 and 2 for $gg \to t\bar{c}$ and $cg \to tZ$, respectively. Other processes have similar Feynman diagrams which can be easily obtained from Figs. 1 and 2. For example, $cg \to tg$ can be straightforwardly obtained from Fig. 1, and $cg \to t\gamma$ can be obtained from Fig. 2 by removing some diagrams with nonexistent vertices. The calculations for these production processes are straightforward. Here we take the calculation of $gg \to t\bar{c}$ as an example. Its amplitude takes the form

$$\frac{g_s^2 m_t^2}{2F_t^2}\frac{v^2 - F_t^2}{v^2} K_{UR}^{tt} K_{UR}^{tc} \epsilon_\mu(k_1)\epsilon_\nu(k_2) \times \sum_i T^i \bar{u}(p_t)\Gamma_i^{\mu\nu} P_R v(p_c), \tag{8}$$

where the sum is over all the Feynman diagrams in Fig. 1, T_i are color factors, $P_R = (1 + \gamma_5)/2$, $k_{1,2}$ denote the momentum of two incoming gluons and $p_{t,c}$ the momentum of outgoing top and anticharm quarks, and $\Gamma_i^{\mu\nu}$ is given by

$$\begin{aligned} &c_1^i p_t^\mu p_t^\nu + c_2^i p_c^\mu p_c^\nu + c_3^i p_t^\mu p_c^\nu + c_4^i p_t^\nu p_c^\mu + c_5^i p_t^\mu \gamma^\nu \\ &+ c_6^i p_c^\mu \gamma^\nu + c_7^i p_c^\nu \gamma^\mu + c_8^i p_t^\nu \gamma^\mu + c_9^i g^{\mu\nu} \\ &+ c_{10}^i \gamma^\mu \gamma^\nu + c_{11}^i p_t^\mu p_t^\nu \not{k}_2 + c_{12}^i p_c^\mu p_c^\nu \not{k}_2 \\ &+ c_{13}^i p_t^\mu p_c^\nu k_2 + c_{14}^i p_t^\nu p_c^\mu \not{k}_2 + c_{15}^i p_t^\mu \gamma^\nu \not{k}_2 \\ &+ c_{16}^i p_c^\mu \gamma^\nu \not{k}_2 + c_{17}^i p_c^\nu \gamma^\mu \not{k}_2 + c_{18}^i p_t^\nu \gamma^\mu \not{k}_2 \\ &+ c_{19}^i g^{\mu\nu} \not{k}_2 + c_{20}^i i\varepsilon^{\mu\nu\alpha\beta}\gamma_\alpha k_{2\beta}. \end{aligned} \tag{9}$$

Here the coefficients c_j^i are obtained by the straightforward calculation of each Feynman diagram in Fig. 1, which are composed of scalar loop functions [20] and can be calculated by using LoopTools [21]. The calculations of the loop diagrams are tedious and the analytical expressions for the coefficients c_j^i are lengthy, so we do not present the explicit expressions for them.

The hadronic cross section at the LHC is obtained by convoluting the parton cross section with the parton distribution functions. In our calculations we use CTEQ6L [22] to generate the parton distributions with the renormalization scale μ_R and the factorization scale μ_F chosen to be $\mu_R = \mu_F = m_t$. To make our estimations more realistic, we applied some kinematic cuts. For example, we require

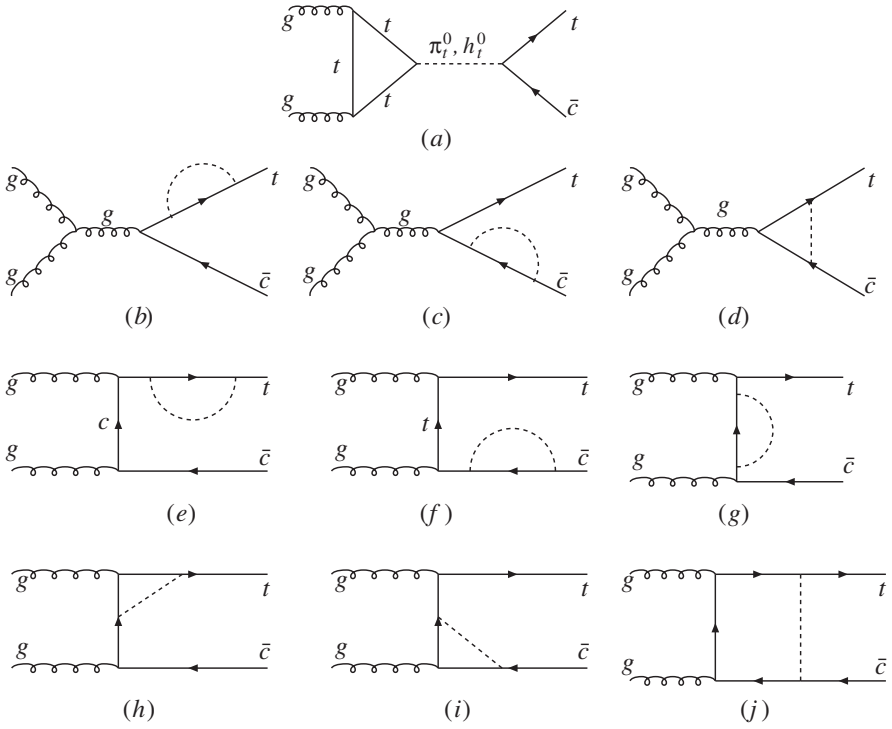

FIG. 1. Feynman diagrams for $gg \to t\bar{c}$ in the TC2 model. The boson in each loop denotes a neutral top pion, top Higgs, or a charged top pion, while the fermion in each loop can be a top or bottom quark depending on the involved boson being neutral or charged.

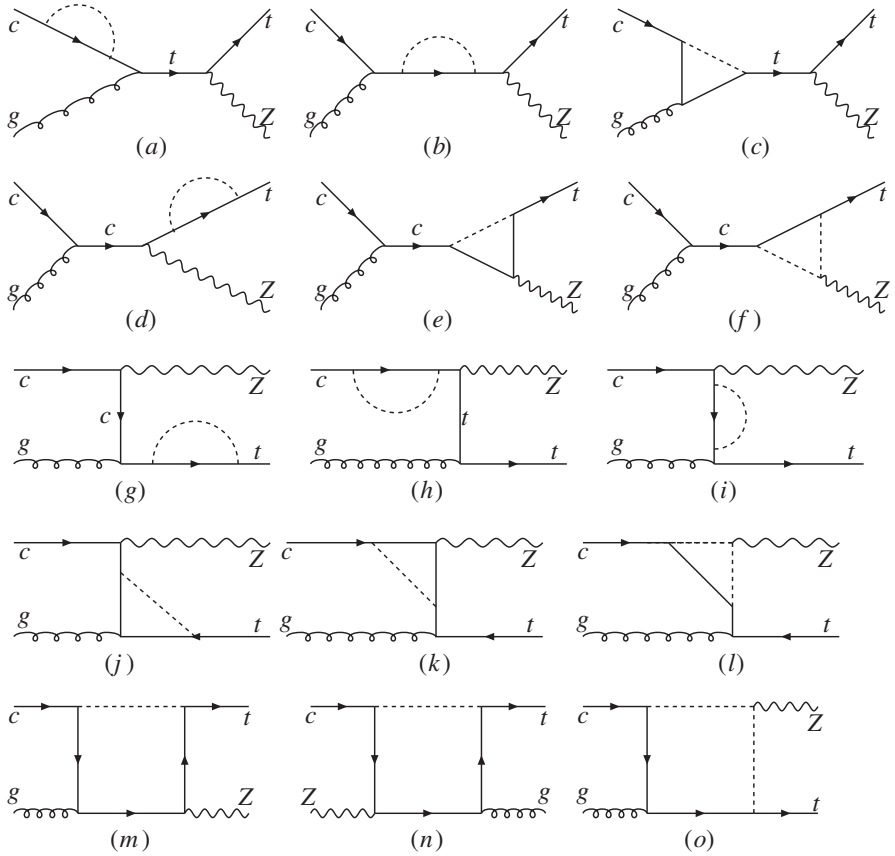

FIG. 2. Feynman diagrams for $cg \to tZ$ in the TC2 model. The boson in each loop denotes a neutral top pion, top Higgs, or a charged top pion, while the fermion in each loop can be a top or bottom quark depending on the involved boson being neutral or charged.

that the transverse momentum of each produced particle larger than 15 GeV and its pseudorapidity less than 2.5 in the laboratory frame. For $cg \to t$ followed by $t \to Wb$, we do not require the top quark exactly on the mass shell and instead we require the invariant mass of the bottom quark and W boson in a region of $m_t - 3\Gamma_t \le M_{bW} \le m_t + 3\Gamma_t$ (Γ_t is the top-quark width). This requirement was used in [23] to investigate the observability of this channel at hadron colliders in the effective Lagrangian framework.

IV. NUMERICAL RESULTS

Since the cross section for each channel is simply proportional to $(K_{UR}^{tc})^2$ as shown in Eq. (8), here we do not show the dependence on K_{UR}^{tc}. We will fix $K_{UR}^{tc} = 0.4$ and show the dependence on M_{TC}. In Fig. 3 we show the hadronic cross section of the production proceeding by the parton-level process $gg \to t\bar{c}$ versus M_{TC}, where the s-channel and non-s-channel contributions are shown separately. From Fig. 3 we see that the contributions are dominated by the s-channel process for a heavy top pion and there exist three regions of M_{TC}. In the range $m_t < M_{TC} < 2m_t$, the cross section is maximal and can reach about 30 pb. The reason is that in this region $t\bar{c}$ is the dominant decay mode of π_t^0 and h_t^0 which can be produced on shell through the s channel. When M_{TC} passes the threshold of $2m_t$ and keeps increasing, the cross section drops quickly since the $t\bar{t}$ is becoming the dominant decay mode of π_t^0 and h_t^0. In the light mass region $M_{TC} < m_t$

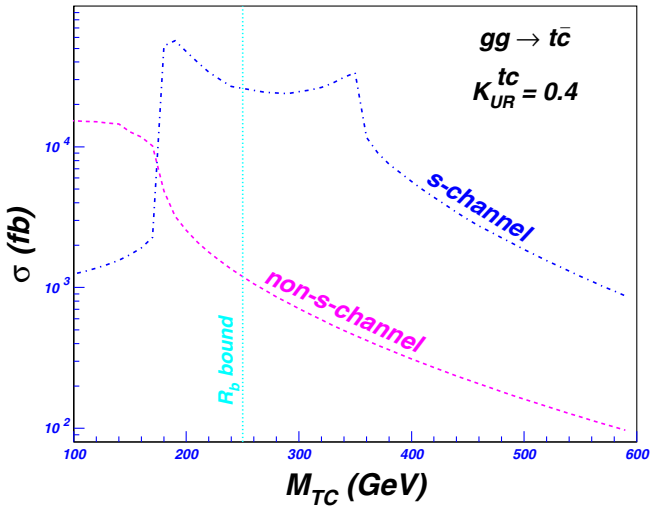

FIG. 3 (color online). The hadronic cross section of the production proceeding through $gg \to t\bar{c}$ versus M_{TC}.

(note that $M_{TC} < 250$ GeV is disfavored by R_b, as commented in Sec. II) the non-s-channel contributions are dominant and the s-channel contributions are suppressed since the top pion and the top Higgs in the s channel cannot be produced on shell.

The total hadronic cross sections for all these processes are plotted in Fig. 4 for comparison. We see that the production proceeding through $gg \to t\bar{c}$ has the largest rate for a heavy top pion. Of course, the productions in the two channels of $gg \to t\bar{c}$ and $cg \to tg$ cannot be distinguished from each other since the charm quark jet cannot be distinguished from the gluon jet. Therefore, the cross sections of these two channels should be summed, which gives a signal of an energetic lepton (electron or muon) plus two jets (one of them is b jet) plus missing energy.

Now we compare the TC2 results with the predictions in the supersymmetric model in Table I. The TC2 results are taken from Fig. 4 for $M_{TC} = 300$ GeV and $K_{UR}^{tc} = 0.4$, while the predictions of the minimal supersymmetric model are the maximal values taken from [9]. The parameters δ_{LL} and δ_{LR} parametrize the mixing between top squarks and charm squarks and their definitions can be found in [9]. We see that for each channel the TC2 allows for a much larger production rate than the minimal supersymmetric model.

In Table I we also list the LHC sensitivity with 100 fb^{-1} integrated luminosity. Such sensitivity for each production channel has been intensively investigated in the literature listed in Table I. Although these sensitivities are based on the effective Lagrangian approach and may be not perfectly applicable to a specified model, we can take them as a rough criteria to estimate the observability of these channels. Comparing these sensitivities with the TC2 results, we see that all the productions can be above the 3σ sensitivity of the LHC for the chosen TC parameters. But for the minimal supersymmetric model, only the prediction for $cg \to t$ is slightly larger than the corresponding LHC sensitivity. Therefore, if these rare processes are observed at the LHC, the TC2 model, rather than supersymmetry, will be favored. Of course, in case of unobservation of these rare productions, the LHC can set meaningful constraints on TC2 parameters.

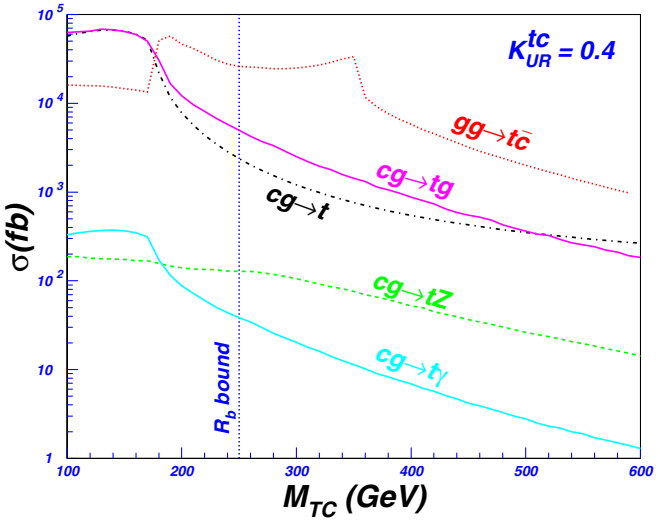

FIG. 4 (color online). The hadronic cross sections of the productions proceeding through the parton-level processes labeled on each curve.

TABLE I. The hadronic cross sections of top-quark FCNC productions in the TC2 and the minimal supersymmetric model. The TC2 results are taken from Fig. 4 for $M_{TC} = 300$ GeV and $K_{UR}^{tc} = 0.4$, while the predictions of the minimal supersymmetric model are the maximal values taken from [9]. The corresponding charge-conjugate channels are also included. The LHC sensitivities in the last column are for 100 fb^{-1} integrated luminosity.

	SUSY		TC2	LHC sensitivity 3σ
	$\delta_{LL} \neq 0$	$\delta_{LR} \neq 0$		
$gg \to t\bar{c}$	240 fb	700 fb	30 pb	1500 fb [24,25]
$cg \to t$	225 fb	950 fb	1.5 pb	800 fb [23]
$cg \to tg$	85 fb	520 fb	3 pb	1500 fb [24,25]
$cg \to t\gamma$	0.4 fb	1.8 fb	20 fb	5 fb [26]
$cg \to tZ$	1.5 fb	5.7 fb	100 fb	35 fb [26]

Note that in Table I we did not list the SM predictions, which have not been calculated in the literature since they must be far below the observable level due to the extremely suppressed top-quark FCNC interactions [1]. Also, we did not list the comparison of TC2 and supersymmetry predictions for various top-quark FCNC decays, which can be found in the last reference of [7]. From there we see that for top-quark FCNC decays the TC2 results are also much larger than supersymmetry predictions. So the potentially large top-quark FCNC interaction is one characteristic of the TC2 model and will serve as a crucial test for this model at future collider experiments.

V. CONCLUSIONS

We evaluated the top-quark FCNC productions in the topcolor assisted technicolor model at the LHC. These productions proceed, respectively, by the parton-level processes $gg \to t\bar{c}$, $cg \to t$, $cg \to tg$, $cg \to tZ$, and $cg \to t\gamma$. We found that the production rates in this model can be much larger than in the supersymmetric model and all the productions can be enhanced above the 3σ sensitivity of the LHC. Since in the minimal supersymmetric model only $cg \to t$ is slightly larger than the corresponding LHC sensitivity, the observation of these processes will imply that the TC2 model is more favored than the supersymmetric model. In case of unobservation of these rare productions, the LHC can set meaningful constraints on TC2 parameters.

ACKNOWLEDGMENTS

J. M. Y. thanks K. Hikasa for helpful discussions and acknowledges the COE program of Japan for supporting a visit in Tohoku University where part of this work is done. This work is supported in part by the Lady Davis Foundation at the Technion, by the Israel Science Foundation (ISF), the National Natural Science Foundation of China under Grant No. 10475107 and No. 10505007, and by the IISN and the Belgian science policy office (IAP V/27).

[1] For the FCNC top-quark decays in the SM, see, G. Eilam, J. L. Hewett, and A. Soni, Phys. Rev. D **44**, 1473 (1991); B. Mele, S. Petrarca, and A. Soddu, Phys. Lett. B **435**, 401 (1998); A. Cordero-Cid *et al.*, Phys. Rev. D **73**, 094005 (2006).

[2] For a recent review, see, e.g., F. Larios, R. Martinez, and M. A. Perez, Int. J. Mod. Phys. A **21**, 3473 (2006).

[3] M. Paulini, arXiv:hep-ex/9701019; J. Incandela, FERMILAB Report No. FERMILAB-CONF-95/237-E, 1995; D. Gerdes, arXiv:hep-ex/9706001; T. J. Lecompte, FERMILAB Report No. FERMILAB-CONF-96/021-E, 1996; A. P. Heinson, arXiv:hep-ex/9605010.

[4] J. A. Aguilar-Saavedra, Acta Phys. Pol. B **35**, 2695 (2004).

[5] For FCNC top-quark decays in the MSSM, see, C. S. Li, R. J. Oakes, and J. M. Yang, Phys. Rev. D **49**, 293 (1994); G. Couture, C. Hamzaoui, and H. Konig, Phys. Rev. D **52**, 1713 (1995); J. L. Lopez, D. V. Nanopoulos, and R. Rangarajan, Phys. Rev. D **56**, 3100 (1997); G. M. de Divitiis, R. Petronzio, and L. Silvestrini, Nucl. Phys. **B504**, 45 (1997); J. M. Yang, B.-L. Young, and X. Zhang, Phys. Rev. D **58**, 055001 (1998); C. S. Li, L. L. Yang, and L. G. Jin, Phys. Lett. B **599**, 92 (2004); M. Frank and I. Turan, Phys. Rev. D **74**, 073014 (2006); J. M. Yang and C. S. Li, Phys. Rev. D **49**, 3412 (1994); J. Guasch and J. Sola, Nucl. Phys. **B562**, 3 (1999); G. Eilam, *et al.*, Phys. Lett. B **510**, 227 (2001); J. L. Diaz-Cruz, H.-J. He, C.-P. Yuan, Phys. Lett. B **179**, 530 (2002); D. Delepine and S. Khalil, Phys. Lett. B **599**, 62 (2004).

[6] For top-charm associated productions in the MSSM, see, G. Eilam, M. Frank, and I. Turan, Phys. Rev. D **74**, 035012 (2006); J. J. Liu, C. S. Li, L. L. Yang, and L. G. Jin, Nucl. Phys. **B705**, 3 (2005); J. Guasch, *et al.*, Nucl. Phys. B, Proc. Suppl. **157**, 152 (2006); J. M. Yang, Ann. Phys. (N.Y.) **316**, 529 (2005); J. Cao, Z. Xiong, and J. M. Yang, Nucl. Phys. **B651**, 87 (2003).

[7] For exotic top production processes in TC2 models, see, J. Cao, Z. Xiong, and J. M. Yang, Phys. Rev. D **67**, 071701 (2003); C. Yue, *et al.*, Phys. Lett. B **496**, 93 (2000); J. Cao, *et al.*, Phys. Rev. D **70**, 114035 (2004); F. Larios and F. Penunuri, J. Phys. G **30**, 895 (2004); J. Cao, *et al.* Eur. Phys. J. C **41**, 381 (2005).

[8] For FCNC top-quark decays in TC2 theory, see, X. L. Wang *et al.*, Phys. Rev. D **50**, 5781 (1994); C. Yue, *et al.*, Phys. Rev. D **64**, 095004 (2001); G. Lu, F. Yin, X. Wang, and L. Wan, Phys. Rev. D **68**, 015002 (2003).

[9] J. Cao, *et al.*, Phys. Rev. D **74**, 031701 (2006); Phys. Rev. D **75**, 075021 (2007).

[10] C. Yue and Z. Zong, J. Phys. G **31**, 401 (2005); W. Xu, X. Wang, and Z. Xiao, arXiv:hep-ph/0612063.

[11] C. T. Hill, Phys. Lett. B **345**, 483 (1995); K. Lane and E. Eichten, Phys. Lett. B **352**, 382 (1995); **433**, 96 (1998); W. A. Bardeen, C. T. Hill, M. Lindner, Phys. Rev. D **41**, 1647 (1990); G. Cvetic, Rev. Mod. Phys. **71**, 513 (1999).

[12] G. Burdman and D. Kominis, Phys. Lett. B **403**, 101 (1997); W. Loniaz and T. Takuch, Phys. Rev. D **62**, 055005 (1999).

[13] H. J. He and C. P. Yuan, Phys. Rev. Lett. **83**, 28 (1999); G. Burdman, Phys. Rev. Lett. **83**, 2888 (1999).

[14] G. Buchalla, G. Burdman, C. T. Hill, and D. Komins, Phys. Rev. D **53**, 5185 (1996).

[15] Tevatron Electroweak Working Group (for the CDF and D0 Collaborations), arXiv:hep-ex/0703034.

[16] R. S. Chivukula, B. Dobrescu, H. Georgi, and C. T. Hill, Phys. Rev. D **59**, 075003 (1999).

[17] W.-M. Yao *et al.*, J. Phys. G **33**, 1 (2006).

[18] Z. Xiao, L. Jia, L. Lu, and G. Lu, Commun. Theor. Phys. **33**, 269 (2000).

[19] C. T. Hill and X. Zhang, Phys. Rev. D **51**, 3563 (1995); C. Yue, Y. P. Kuang, X. Wang, and W. Li, Phys. Rev. D **62**, 055005 (2000).

[20] G. 't Hooft and M. J. G. Veltman, Nucl. Phys. **B153**, 365 (1979).

[21] T. Hahn and M. Perez-Victoria, Comput. Phys. Commun. **118**, 153 (1999); T. Hahn, Nucl. Phys. B, Proc. Suppl. **135**, 333 (2004).

[22] J. Pumplin, *et al.*, J. High Energy Phys. 02 (2006) 032.

[23] M. Hosch, K. Whisnant, B. L. Young, Phys. Rev. D **56**, 5725 (1997).

[24] T. Han, *et al.*, Phys. Rev. D **58**, 073008 (1998).

[25] T. Stelzer, Z. Sullivan, and S. Willenbrock, Phys. Rev. D **58**, 094021 (1998).

[26] F. del Aguila and J. A. Aguilar-Saavedra, Nucl. Phys. **B576**, 56 (2000).